Synthesis, Structure, and Magnetic Properties of Two New Ferromagnetic/Antiferromagnetic One-Dimensional Nickel(II) Complexes. Magnetostructural Correlations

Montserrat Monfort, Immaculada Resino, and Joan Ribas*

Departament de Química Inorgànica, Universitat de Barcelona, Diagonal 647, 08028 Barcelona, Spain

Xavier Solans and Merce Font-Bardia

Departament de Cristalografia i Mineralogia, Universitat de Barcelona, Martí i Franqués, s/n, 08028 Barcelona, Spain

Pierre Rabu and Marc Drillon

Institut de Physique et Chimie des Matériaux de Strasbourg, UMR7504, 23 rue du Loess, 67037 Strasbourg, France

Received November 24, 1999

Two new one-dimensional nickel(II) complexes were synthesized and characterized: [Ni(*N*,*N*-dimethylethylenediamine)$(N_3)_2$] (**1**) and [Ni(2-aminoethylpyridine)$(N_3)_2$] (**2**). The crystal structures of **1** and **2** were solved. Complex **1** crystallizes in the monoclinic system, space group $P2_1/n$ with $a = 10.569(2)$ Å, $b = 7.331(4)$ Å, $c = 12.9072(8)$ Å, $\beta = 111.324(10)°$, and $Z = 4$. Complex **2** crystallizes in the monoclinic system, space group $P2_1/c$ with $a = 12.299(5)$ Å, $b = 14.307(2)$ Å, $c = 12.604(3)$, $\beta = 106.72(2)°$, and $Z = 4$. The two complexes are similar and may be described as one-dimensional systems with double-azido-bridged ligands in end-to-end and end-on coordination alternatively. The end-on moiety is almost identical for **1** and **2**, but the end-to-end moiety is different in each structure: for **1** this part is almost planar but for **2** is nonplanar. In both cases the Ni atoms are situated in similar distorted octahedral environments. The magnetic properties of the two compounds were studied by susceptibility measurements vs temperature. The χ_M vs T plots for **1** and **2** show a global antiferromagnetic behavior with a maximum near room temperature for **1** and at very low temperature for **2**. J values for **1** and **2** were deduced from the spin Hamiltonian $-\sum(J_1S_iS_{i+1} + J_2S_{i+1}S_{i+2})$. The computational method was based on the numerical solution for finite systems of increasing size. J values for **1** were $J_1 = -187$ cm^{-1} and $J_2 = +77$ cm^{-1} and for **2** $J_1 = -28$ cm^{-1} and $J_2 = +73$ cm^{-1}. The positive values correspond to end-on azido ligands and the negative values to end-to-end azido ligands. Since the geometries of the $[Ni(N_3)]_2$ moieties involving the end-on azido ligands are almost the same in the two structures, the ferromagnetic coupling is nearly identical in the two compounds, while the significantly different antiferromagnetic couplings reflect the near planarity of the end-to-end $Ni_2(N_3)_2$ fragment in **1** and its twisted geometry in **2**.

Introduction

One-dimensional magnetic systems have been studied from both experimental and theoretical points of view.[1−3] The large number of antiferromagnetic alternating chains contrasts with the paucity of alternating chains with J_i and J_{i+1} of different signs (ferro- and antiferromagnetic). With Cu(II), the best documented systems are $[CuCl_3$(4-Bzpip)] (Bzpip = 4-benzylpiperidinium),[4] [Cu(hfac)(TEMPOL)] (hfac = hexafluoroacetylacetonate and TEMPOL = 4-hydroxy-2,2,6,6-tetramethylpiperidinyl-*N*-oxy),[5] [Cu(TIM)$CuCl_4$] (TIM = 2,3,9,10-tetramethyl-1,3,8,10-tetraenecyclo-1,4,8,11-tetrazatetradecane),[6] $[Cu_2(bpm)_2(H_2O)_2(NO_3)_2]\cdot 2H_2O$ (bpm = 2,2′-bipyrimidine) and related compounds,[7] [{Cu_2(Me$_2$Eten)$_2(N_3)_2(\mu_{1,1,3}$-$N_3)_2$}] (Me$_2$eten = *N*,*N*-dimethyl-*N*′-ethylethylenediamine),[8] and [Cu(4,4′-dimethylbipyridine)$(N_3)_2$].[9] For this kind of $S = 1/2$ ferromagnetic/antiferromagnetic (F/AF) system, Borrás et al.[10] have recently presented an ensemble of rational

(1) (a) *Extended Linear Chains Compounds*; Miller, J. S., Ed.; Plenum: New York, 1983. (b) Bonner, J. C. In *Magneto-Structural Correlations in Exchange Coupled Systems;* Willet, R. D., Gatteschi, D., Kahn, O., Eds.; NATO ASI Series 140; Reidel: Dordrecht, The Netherlands, 1985; p 157.
(2) *Organic and Inorganic Low-Dimensional Crystalline Materials*; Delhaes, P., Drillon, M., Eds.; NATO ASI Series 168; Plenum: New York, 1987.
(3) *Magnetic Molecular Materials*; Gatteschi, D., Kahn, O., Miller, J. S., Palacio, F., Eds.; Kluwer Academic Publishers: Dordrecht, The Netherlands, 1991.
(4) De Groot, H. J. M.; de Jongh, L. J.; Willet, R. D.; Reedijk, *J. Appl. Phys.* **1982**, *53*, 8038.
(5) Benelli, C.; Gatteschi, D.; Carnegie, D. W.; Carlin, R. L. *J. Am. Chem. Soc*. **1985**, *107*, 2560.
(6) Vasilevesky, L.; Rose, N. R.; Stenkamp, R.; Willet, R. D. *Inorg. Chem.* **1991**, *30*, 4082.
(7) De Munno, G.; Julve, M.; Lloret, F.; Faus, J.; Verdaguer, M.; Caneschi, A. *Inorg. Chem*. **1995**, *34*, 157.
(8) Escuer, A.; Font-Bardía, M.; Peñalba, E.; Solans, X.; Vicente R. *Polyhedron* **1998**, *18*, 211.
(9) Shen, H.-Y.; Bu, W.-M.; Gao, E.-Q.; Liao, D.-Z.; Jiang, Z.-H.; Yan, S.-P.; Wang, G.-L. *Inorg. Chem*. **2000**, *39*, 396.
(10) Borrás-Almenar J. J.; Coronado, E.; Curely, J.; Georges, R.; Gianduzzo, J. C. *Inorg. Chem*. **1994**, *33*, 5171.

10.1021/ic991366j CCC: $19.00
Published on Web 05/24/2000

Table 1. Crystallographic Data for **1** and **2**

	1	**2**		**1**	**2**
empirical formula	$C_4H_{12}N_8Ni$	$C_7H_{10}N_8Ni$	V, Å^3	931.6(5)	2124.1(10)
fw	230.93	264.94	Z	4	4
temp, K	293	293	λ(Mo Kα), Å	0.710 69	0.710 69
space group	$P2_1/n$	$P2_1/c$	d_{calcd}, g·cm^{-3}	1.646	1.657
a, Å	10.569(2)	12.299(5)	μ(Mo Kα), mm^{-1}	2.053	1.813
b, Å	7.331(4)	14.307(2)	R^a	0.0335	0.0317
c, Å	12.9072(8)	12.604(3)	$R_w{}^b$	0.0849	0.0936
α, deg	90.00	90.00			
β, deg	111.324(10)	106.72(2)			
γ, deg	90.00	90.00			

^{a} $R = \Sigma||F_o| - |F_c||/\Sigma|F_o|$. ^{b} $R_w = [\Sigma w(|F_o|^2 - |F_c|^2)/\Sigma w|F_o|^2]^{1/2}$.

unified expressions for the magnetic susceptibility data as a function of $\alpha = J_2/J_1$. J_1 and J_2 are the coupling constants of the AF and F exchange interactions, respectively. With Ni(II) the best documented systems are [Ni(dmen)(μ-N_3)$_2$][11] (dmen = *N*,*N*-dimethylethylenediamine), [Ni(aep)(μ-N_3)$_2$][11] (aep = 2-aminoethylpyridine), [Ni(bpy)(μ-N_3)$_2$],[12] [{Ni$_2$(Medien)$_2$($\mu_{1,1}$-N_3)$_2$($\mu_{1,3}$-N_3)}$_n$](ClO$_4$)$_n$,[13] and [Ni(4,4′-dimethylbipyridine)-(N_3)$_2$].[9] Escuer et al.,[13] Borrás et al.,[14] and Esposito et al.[15] have studied systems of this kind from different viewpoints and have developed rational unified expressions for the magnetic susceptibility data. The treatment proposed by Exposito et al. is based on the transfer matrix method, which implies that only the *z* component of the spins is considered (Ising model). This approximation is not appropriate for the nickel(II) ion, whose local anisotropy (D) does not exceed a few wavenumbers. With Mn^{II} several alternating chains (F/AF) have been reported to date: [Mn(bipy)(μ-N_3)$_2$],[16] [Mn(3-Et,4-Mepy)(μ-N_3)$_2$][17] (3-Et,4-Mepy = 3-ethyl-4-methylpyridine), [Mn(4,4′-dimethylbipyridine)(N_3)$_2$],[9] [Mn(bpm)(N_3)$_2$]$_n$,[18] and [Mn(3-bzpy)$_2$(N_3)$_2$]$_n$ (3-bzpy = 3-benzoylpyridine).[19] It is interesting to pay attention that simple ligands such as azido bridges can be used to build one-dimensional magnetic systems with regular alternation of ferro- and antiferromagnetic couplings. The azido ligand has two main coordination modes: *end-to-end* (or 1,3) which normally gives antiferromagnetic coupling and *end-on* (1,1) which normally gives ferromagnetic coupling.[20] Focusing our interest on systems of this kind, we therefore synthesized two new ferro- antiferromagnetic alternating chains with an azido bridging ligand and terminal chelating amines: [Ni(dmen)(μ-N_3)$_2$] (**1**) and [Ni(aep)(μ-N_3)$_2$] (**2**) (dmen = *N*,*N*-dimethylethylenediamine; aep = 2-aminoethylpyridine). A preliminary communication concerning the structure and magnetic investigations of compounds **1** and **2** was published elsewhere.[11]

Experimental Section

Caution! *Azide complexes of metal ions are potentially explosive. Only a small amount of material should be prepared, and it should be handled with caution.*

Synthesis of the New Complexes. [Ni(dmen)(μ-N_3)$_2$] (1) and [Ni(aep)(μ-N_3)$_2$] (2). An aqueous solution (25 mL) of NaN_3 (0.26 g, 4 mmol) was added to an aqueous solution (25 mL) of Ni(NO$_3$)$_2$·6H$_2$O (0.58 g, 2 mmol) and dmen (0.18 g, 2 mmol) or aep (0.27 g, 2 mmol). After filtration to remove any impurity, the solutions were left undisturbed, and well-formed green crystals of **1** and **2** were obtained after several days. The yield was almost quantitative. Elementary analyses (C, N, H, Ni) were consistent with the formulation.

Crystal Structure Determination. Crystals of **1** and **2** were selected and mounted on an Enraf-Nonius CAD4 diffractometer. Unit cell parameters were determined from automatic centering of 25 reflections ($12° < \theta < 21°$) for **1** and **2** and refined by least-squares methods. Intensities were collected with graphite-monochromatized Mo Kα radiation, using the $\omega/2\theta$ scan technique. For **1** 2815 reflections were measured in the range $2.14° < \theta < 29.9°$; 2324 reflections were assumed as observed applying the condition $I > 2\sigma(I)$. For **2**, 6170 reflections were measured in the range $1.73° < \theta < 29.99°$; 6119 reflections were assumed as observed applying the condition $I > 2\sigma(I)$. Three reflections were measured every 2 h as orientation and intensity control; significant intensity decay was not observed. Lorentz and polarization corrections were made for both compounds. The crystallographic data are shown in Table 1. The crystal structures were solved by Patterson synthesis with the SHELX computer program[21] and refined by full-matrix least-squares methods using the SHELX-93 computer program.[22] The function minimized was $\Sigma w[|F_o|^2 - |F_c|^2]^2$, where $w = [\sigma^2(I) + (0.0988P)^2 + 0.1576P]^{-1}$ and $P = (|F_o|^2 + 2|F_c|^2)/3$, for **1**, and $\Sigma w[|F_o|^2 - |F_c|^2]^2$, where $w = [\sigma^2(I) + (0.1355P)^2 + 3.1152P]^{-1}$ and $P = (|F_o|^2 + 2|F_c|^2)/3$ for **2**. f, f', and f'' were taken from ref 23. Twelve and eleven hydrogen atoms were located from a difference synthesis and refined with an overall isotropic temperature factor for **1** and **2**, respectively. For **2**, nine hydrogen atoms were computed and refined with an overall isotropic temperature factor using a riding model. For **1** the final R factor was 0.0335 ($R_w = 0.0849$) for all observed reflections. A total of 153 parameters were refined, the maximum shift/esd = 0.16, maximum and minimum peaks in the final difference synthesis were +0.722 and −1.146 e Å^{-3}, respectively. For **2** the final R factor was 0.0317 ($R_w = 0.0936$) for all observed reflections. A total of 324 parameters were refined, the maximum shift/esd = 0.003, and maximum and minimum peaks in the final difference synthesis were +0.697 and −0.677 e Å^{-3}. Final atomic coordinates for **1** and **2** are given in Tables 2 and 4, respectively.

Physical Measurements. Magnetic measurements were carried out on polycrystalline samples with a SQUID magnetometer (Métronique).

(11) Ribas, J.; Monfort, M.; Ghosh, B. K.; Solans, X.; Font-Bardía, M. *J. Chem. Soc., Chem. Commun*. **1995**, 2375.
(12) Viau, G.; Lombardi, M. G.; De Munno, G.; Julve, M.; Lloret, M.; Faus, J.; Caneschi, A.; Clemente-Juan, J. M. *Chem. Commun*. **1997**, 1195.
(13) Escuer, A.; Vicente, R.; El Fallah, M. S.; Kumar, S. B.; Mautner, F. A.; Gatteschi, D. *J. Chem. Soc., Dalton Trans*. **1998**, 3905.
(14) Borrás-Almenar, J. J.; Clemente-Juan, J. M.; Coronado, E.; Lloret, F. *Chem. Phys. Lett*. **1997**, *275*, 79.
(15) (a) D'Auria, A. C.; Esposito, U.; Esposito, F.; Gatteschi, D.; Kamieniarz, G.; Walcerz, S. *J. Chem. Phys*. **1998**, *109*, 1613. (b) Esposito, F.; Kamieniarz, G. *Phys. Rev. B* **1998**, *57*, 7431.
(16) (a) Cortés, R.; Lezama, L.; Pizarro, J.L.; Arriortua, M. I.; Solans, X.; Rojo, T. *Angew. Chem., Int. Ed. Engl*. **1994**, *33*, 2488. (b) Cortés, R.; Drillon, M.; Solans, X.; Lezama, L.; Rojo, T. *Inorg. Chem*. **1997**, *36*, 677.
(17) Abu-Youssef, M. A. M.; Escuer, A.; Goher, M. A. S., Mautner, F. A.; Vicente. R. *Eur. J. Inorg. Chem*. **1999**, 687.
(18) Tang, L.-F.; Zhang, L.; Li, L.-C.; Cheng, P.; Wang, Z.-H.; Wang, J.-T. *Inorg. Chem*. **1999**, *38*, 6326.
(19) Abu-Youssef, M. A. M.; Escuer, A.; Gatteschi, D.; Goher, M. A. S.; Mautner, F. A.; Vicente, R. *Inorg. Chem*. **1999**, *38*, 5716.
(20) Ribas. J.; Escuer, A.; Monfort, M.; Vicente, R.; Cortés, R.; Lezama, L.; Rojo, T. *Coord. Chem. Rev*. **1999**, *193*−*195*, 1027.
(21) Sheldrick, G. M. *Acta Crystallogr*. **1990**, *A46*, 467.
(22) Sheldrick, G. M. A computer program for crystal structure determination. University of Cambridge, U.K., 1976.
(23) *International Tables for X-ray Crystallography*; Kynoch Press: Birmingham, England, 1976.

Table 2. Atomic Coordinates ($\times 10^4$) and Equivalent Isotropic Displacement Parameters (Å^2 $\times$ 10^3) for Significant Atoms of **1**[a]

	x	*y*	*z*	*U*(eq)
Ni	953(1)	1735(1)	39(1)	29(1)
N(1)	−424(2)	784(2)	806(1)	36(1)
N(2)	−35(2)	1014(2)	1794(1)	39(1)
N(3)	325(3)	1274(4)	2736(2)	65(1)
N(4)	−610(2)	3022(2)	−1251(1)	43(1)
N(5)	962(1)	5479(2)	1146(1)	30(1)
N(6)	1376(2)	4018(2)	1114(1)	46(1)
N(7)	2559(2)	427(2)	1224(1)	40(1)
N(8)	2499(2)	2672(2)	−575(1)	42(1)

[a] *U*(eq) is defined as one-third of the trace of the orthogonalized U_{ij} tensor.

Table 3. Selected Bond Lengths (Å) and Angles (deg) for **1**[a]

Ni−N(4)	2.096(2)	Ni−N(8)	2.171(2)
Ni−N(1)A	2.114(2)	Ni−NiA	3.224(1)
Ni−N(6)	2.115(2)	Ni−NiB	5.180(1)
Ni−N(1)	2.152(2)		
N(1)A−Ni−N(1)	81.83(6)	NiA−N(1)−Ni	98.17(6)
N(2)−N(1)−NiA	126.51(12)	N(5)B−N(4)−Ni	121.10(12)
N(2)−N(1)−Ni	114.54(12)	N(5)−N(6)−Ni	139.37(12)

[a] Symmetry transformations used to generate equivalent atoms: (A) $-x, -y, -z$; (B) $-x, -y + 1, -z$.

Table 4. Atomic Coordinates ($\times 10^4$) and Equivalent Isotropic Displacement Parameters (Å^2 $\times$ 10^3) for Significant Atoms of **2**[a]

	x	*y*	*z*	*U*(eq)
Ni(1)	151(1)	450(1)	3881(1)	29(1)
Ni(2)	4230(1)	44(1)	3720(1)	27(1)
N(1)	1259(2)	−689(2)	3827(2)	37(1)
N(2)	1957(2)	−630(2)	3353(2)	31(1)
N(3)	2638(2)	−585(2)	2885(2)	37(1)
N(4)	1373(3)	1418(2)	3631(3)	45(1)
N(5)	2361(2)	1307(2)	3907(2)	31(1)
N(6)	3366(2)	1212(2)	4177(2)	37(1)
N(7)	950(2)	481(2)	5636(2)	37(1)
N(8)	1246(3)	1220(2)	6051(2)	44(1)
N(9)	1532(5)	1943(3)	6435(4)	90(2)
N(10)	4226(2)	−581(2)	5259(2)	34(1)
N(11)	3883(2)	−1348(2)	5372(2)	36(1)
N(12)	3512(3)	−2066(2)	5491(4)	64(1)
N(13)	−860(2)	1580(2)	4040(2)	39(1)
N(14)	−653(2)	337(2)	2171(2)	36(1)
N(15)	5059(2)	−1135(2)	3400(2)	36(1)
N(16)	4379(2)	704(2)	2283(2)	32(1)

[a] *U*(eq) is defined as one-third of the trace of the orthogonalized U_{ij} tensor.

The magnetic field was approximately 500 Oe. The diamagnetic corrections were estimated from Pascal constants.

Results and Discussion

Description of the Structures. Single-crystal X-ray determination of **1** and **2** (Figures 1 and 2) established that they are similar but also show significant differences. Both structures consist of distorted nickel octahedra linked by two types of azido bridges in alternation: EO and EE. The EE and EO bridges are propagated with a mutual perpendicular alignment, producing a net one-dimensional chain. The Ni−N(azido) bond distances are characteristic of bridging azido−nickel(II) complexes (Tables 3 and 5). The main difference between the complexes is in the EE [Ni(μ-N$_3$)$_2$Ni] fragment: in **1** the azido bridging ligands form a plane. The Ni is 0.069 Å from the (N$_3$)$_2$ plane. This (N$_3$)$_2$ planar structure is characteristic of all polynuclear complexes with double EE azido bridges. Only in one case is this planarity not observed: the double-bridged moiety in the $(-Ni-(N_3)_2-Ni-N_3-)_n$ alternating chain, in which the two azido bridging ligands are crossed.[24] In **2** the structure of this [Ni(μ-N$_3$)$_2$Ni] fragment is not planar (Figure 2). The N(3)Ni(2)N(6)N(5)N(4) atoms form a plane, while N(2), N(1), and Ni(1) are clearly separated from this plane. The distances to this plane are, for example, Ni(1)−plane = 1.32 Å and N(1)−plane = 1.62 Å. Other differences between **1** and **2** are less important: the Ni−N−Ni angle in the EO fragment is 98° for **1** and 99° for **2**, which are slightly lower than those (102−

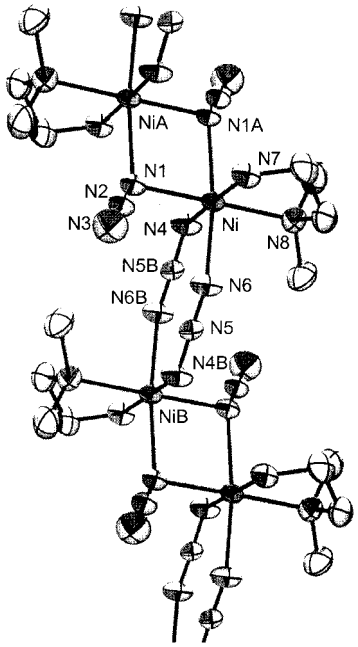

Figure 1. Molecular structure with the atom labeling scheme for [Ni(*N*,*N*-dimethylethylenediamine)(N$_3$)$_2$] (**1**). Ellipsoids at the 50% probability level.

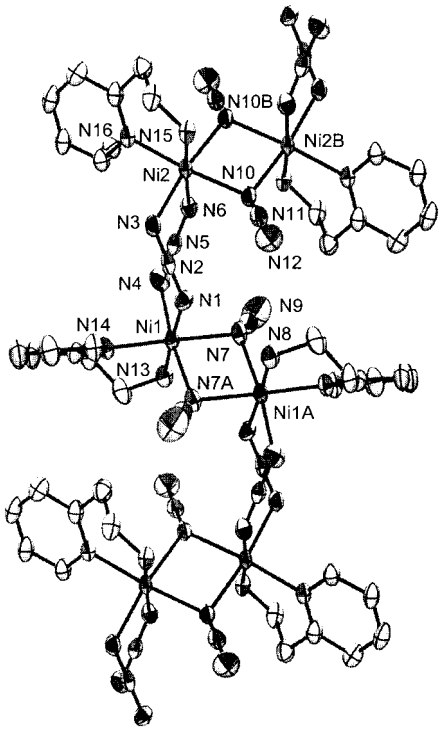

Figure 2. Molecular structure with the atom labeling scheme for [Ni(2-aminoethylpyridine)(N$_3$)$_2$] (**2**). Ellipsoids at the 50% probability level.

(24) Vicente, R.; Escuer, A.; Ribas J.; Solans X. *Inorg. Chem.* **1992**, *31*, 1726.

Table 5. Selected Bond Lengths (Å) and Angles (deg) for **2**[a]

Ni(1)−N(7)A	2.110(3)	Ni(2)−N(10)B	2.108(3)
Ni(1)−N(4)	2.132(3)	Ni(2)−N(10)	2.137(3)
Ni(1)−N(1)	2.138(3)	Ni(2)−N(3)	2.138(3)
Ni(1)−N(7)	2.147(3)	Ni(2)−N(6)	2.146(3)
N(4)−Ni(1)−N(1)	90.44(11)	N(5)−N(6)−Ni(2)	124.4(2)
N(7)A−Ni(1)−N(7)	81.76(11)	N(8)−N(7)−Ni(1)A	125.1(3)
N(10)B−Ni(2)−N(10)	80.55(11)	N(8)−N(7)−Ni(1)	117.5(2)
N(3)−Ni(2)−N(6)	90.34(11)	Ni(1)A−N(7)−Ni(1)	98.24(11)
N(2)−N(1)−Ni(1)	121.6(2)	N(11)−N(10)−Ni(2)B	123.1(2)
N(2)−N(3)−Ni(2)	117.9(2)	N(11)−N(10)−Ni(2)	125.7(2)
N(5)−N(4)−Ni(1)	125.6(2)	Ni(2)B−N(10)−Ni(2)	99.45(11)

[a] Symmetry transformations used to generate equivalent atoms: (A) $-x, -y, -z + 1$; (B) $-x + 1, -y, -z + 1$.

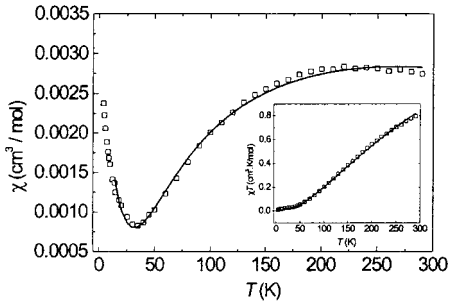

Figure 3. Experimental and calculated variations of the magnetic susceptibility versus temperature for [Ni(*N*,*N*-dimethylethylenediamine)-$(N_3)_2$] (**1**).

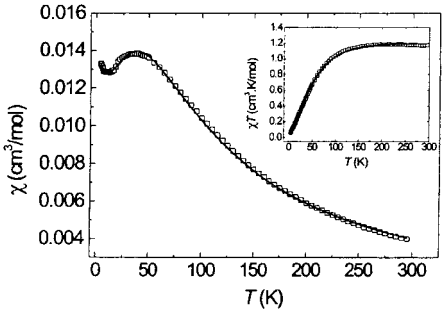

Figure 4. Experimental and calculated variations of the magnetic susceptibility versus temperature for [Ni(2-aminoethylpyridine)$(N_3)_2$] (**2**).

104°) reported for other F dinuclear or one-dimensional nickel(II) complexes,[20] but much higher (ca. 25°) than that found for the triple EO bridge system.[25]

Magnetic Studies. The magnetic behavior of compound **1** is shown in Figure 3. Upon cooling, the $\chi_M T$ (inset) indicates strong antiferromagnetic behavior characterized by a steep gradient from 0.8 cm^3 mol^{-1} K at 298 K. The susceptibility shows a smooth maximum around 225 K at about 0.0028 cm^3 mol^{-1} and a strong decrease to 0.000 75 cm^3 mol^{-1} at 25 K. The sharp increase in χ_M to 0.0024 cm^3 mol^{-1} at 4 K may be attributed to paramagnetic impurities. The magnetic behavior of compound **2** is shown in Figure 4. The $\chi_M T$ product increases very slightly from 300 to 170 K. The value of the Curie constant $C = 1.1624$ K cm^3 mol^{-1} ($\Theta = 3.19$ K) agrees well with that expected for the nickel(II) ions ($S = 1$). Below 170 K, the $\chi_M T$ product decreases to zero with temperature, indicating global antiferromagnetic behavior. Accordingly, the magnetic susceptibility has a maximum at about 40 K. The increase in χ_M at very low temperature may be interpreted as a paramagnetic tail due to isolated nickel(II), which is common in molecular systems. Simulation and fitting of the magnetic susceptibility of both compounds was carried out to calculate the exchange interactions between nearest neighbors along the nickel(II) chains. Taking into account the structural features, these compounds may be viewed as a collection of $S = 1$ spin chains. The nature and geometry of the azido bridges suggest an alternation of ferromagnetic (J_1) and antiferromagnetic (J_2) interactions:

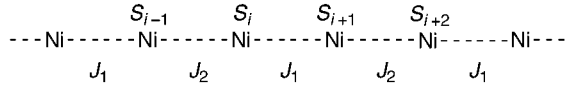

The corresponding spin Hamiltonian of the system is written as

$$H = -\sum(J_1 S_i S_{i+1} + J_2 S_{i+1} S_{i+2}) - D\sum S_z^2 - g\mu_b \sum SH$$

where the S_i hold for the spin operators, D is the zero-field splitting for nickel(II) ion, and H is the applied field. The g factor is assumed to be identical for all the spin carriers. The computational method was based[26,27] on the numerical solutions of H for finite systems of increasing size. The border effects are ruled out by considering a ring of N spins. In this approach, only rings with N being a multiple of 4 may be considered to avoid frustration effects, as shown below:

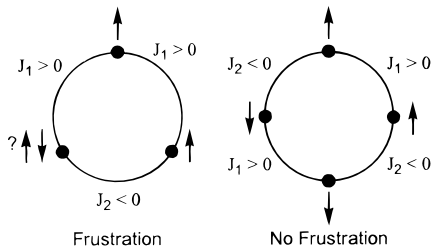

The computing time and memory size necessary to achieve calculations and fits using this model increase considerably with the size of the system. Thus, the calculations were limited to eight $S = 1$ spin rings to fit the experimental data.[28] Finally, a paramagnetic impurity, giving the increase of the susceptibility at low temperature, was taken into account in the expression of the susceptibility as follows:

$$\chi_M = (1 - \rho)\chi_{M(chain)}^{J_1,J_2,g,D}(T) + \rho g^2 S(S+1)/8T$$

where $\chi_{M(chain)}^{J_1,J_2,D,g}$ is the susceptibility of the chain assuming a paramagnetic nickel(II) contribution.

Despite the short chain length used for the calculation, the experimental data are well fitted with this model (Figures 3 and 4). The best values of the refined parameters are given in Table 6.

As expected, the experimental behavior corresponds well to the alternation of ferromagnetic (J_1) and antiferromagnetic (J_2) interactions along the chains. For compound **2**, J_1 is twice the absolute value of J_2, and the refined g factor is in agreement with common values found in the literature for nickel(II).[29]

(25) Ribas, J.; Monfort, M.; Ghosh, B. K.; Solans, X. *Angew. Chem., Int. Ed. Engl.* **1994**, *33*, 2087.
(26) Weng, C. Y. Ph.D. Thesis, Carnegie-Mellen University, 1968.
(27) Ribas, J.; Monfort, M.; Resino, I.; Solans, X.; Rabu, P.; Maingot, F.; Drillon, M. *Angew. Chem., Int. Ed. Engl*. **1996**, *35*, 21 and references therein.
(28) The fits were carried out by using the MINUIT function minimization program of the CERN program library, CERN, Geneva, Switzerland; the C98 vectorial computer of IDRIS, Orsay, France, was used for the calculations involving up to 1107 × 1107 matrixes.
(29) Carlin, R. L. *Magnetochemistry*; Springer-Verlag: Berlin, 1986.

Table 6. The Best Refined Values of the Magnetic Exchange Parameters

compd	D(cm^{-1})	J_1(cm^{-1})	J_2(cm^{-1})	g	par[b] (%)	R[c]
1	0[a]	$+77 \pm 2$	-187.11 ± 1	2.46	1.1	3×10^{-3}
2	0.21 ± 0.21	$+73 \pm 5$	-28.5 ± 0.2	2.11	3.2	6×10^{-3}

[a] Fixed at 0. [b] Paramagnetic impurities. [c] $R = \sum[(\chi_{exp} - \chi_{calcd})^2]/\chi_{exptl}^2$.

Concerning the zero-field splitting, the refined value of D is nearly zero. In fact, the presence of a paramagnetic impurity effect strongly affects the significance of this parameter, which is actually efficient in the low-temperature region. This problem is obvious for compound **1**, for which the refinement of D was unsuccessful within a range of physical significance (i.e., -15 K $< D <$ $+15$ K).[29] Thus, the fit of the experimental susceptibility for this compound was carried out for fixed D values. It appears that the values of the interactions vary only within a few kelvin for the different values of D. Taking into account the result obtained for the other compound, the best parameters refined for $D = 0$ K are given in Table 6. As the main result, the ferromagnetic interaction J_1 is quite unchanged compared to that of compound **1**, but the antiferromagnetic interaction (J_2) is much stronger, as could be deduced from the high-temperature maximum of χ_M. Finally, the g factor is refined to a high value. It may also be linked to the paramagnetic contribution. In fact, as shown in the expression of the corrected susceptibility above, g acts as a scaling factor and can involve small errors on several experimental parameters (calibration and sample mass, for instance).

Magnetostructural Correlations. With regard to the antiferromagnetic part (EE azido bridges), the most interesting feature is the relative position of the two azido bridges in the Ni$-(\mu$-N$_3)_2-$Ni fragment. In **1**, as in most structures with double azido bridges, the two pseudohalides are parallel, but in **2**, these two azido ligands are not parallel, as indicated above. As demonstrated by Vicente et al. the more planar the structure, the higher the antiferromagnetic coupling.[30] This kind of distortion, when symmetrical, has been named τ distortion.[30] For $\tau = 0°$ the AF coupling is maximum, and for $\tau = 30°$ an accidental orthogonality is found; the coupling could be ferromagnetic. The nonparallelism of the azido ligands in **2** is not symmetrical; thus, it is not possible to draw the τ angle, but the deviation of the parallelism is very marked, and it is probably responsible for the change in the J (AF) values: from -187 to -28 cm^{-1}.

The ferromagnetic coupling is very similar for complexes **1** and **2** (Table 6). The Ni$-$N$-$Ni angles are also very similar: 98.18° for **1** and 98.24° for **2**. Ruiz et al.[31] have developed a density functional study for the magnetic coupling in end-on azido-bridged transition-metal complexes. For Ni^{II} complexes, the interaction is predicted to be ferromagnetic for all the range of Ni$-$N$-$Ni angles explored (from 80° to 110°), with J increasing with increasing angle, yielding a maximum at $\theta = 104°$.[31] The influence of the *out-of-plane* displacement of the azido group has also been analyzed. The effect of this structural parameter on the exchange coupling is very small.

Acknowledgment. This work was financially supported by the Dirección General de Investigación Científica y Técnica (Spanish Government), Grant No. PB96/0163.

Supporting Information Available: Two X-ray crystallographic files, in CIF format. This material is available free of charge via the Internet at http://pubs.acs.org.

IC991366J

(30) Vicente, R.; Escuer, A. *Polyhedron* **1995**, *14*, 2133.
(31) Ruiz, E.; Cano, J.; Alvarez, S.; Alemany, P. *J. Am. Chem. Soc.* **1998**, *120*, 11122.